

Highly Efficient Waveform Acquisition Condition in Equivalent-Time Sampling System

Yuto Sasaki, Yujie Zhao, Anna Kuwana, Haruo Kobayashi

Division of Electronics and Informatics, Gunma University, Kiryu, 376-8515, Japan

t14304053@gunma-u.ac.jp, t181d041@gunma-u.ac.jp, kuwana.anna@gunma-u.ac.jp, koba@gunma-u.ac.jp

Abstract—This paper describes the optimal waveform acquisition condition between the measured waveform repetitive frequency (f_{sig}) and the sampling clock frequency (f_{CLK}) in an equivalent-time sampling system, when the measured waveform is periodic. We have obtained that in the case of $f_{CLK} / f_{sig} = 1.6180..$ or the golden ratio, a waveform missing phenomenon for the equivalent-time sampling can be avoided and highly efficient waveform acquisition sampling can be realized. We consider that this can be explained using the relationship to the golden section search algorithm. This paper presents its theoretical consideration and simulation results, and we consider that these results can be utilized in several LSI testing applications such as an ADC histogram testing method using a sine wave input and a timing measurement circuit design besides the equivalent-time sampling system.

Keywords—equivalent-time sampling; sampling oscilloscope; waveform missing; golden ratio; golden section search; ADC histogram testing method

I. INTRODUCTION

A sampling oscilloscope displays wideband waveforms with a relatively low frequency sampling clock using an equivalent-time sampling technique, when the waveform is repetitive [1-4]. This measurement method can be beyond the limitation of the Nyquist sampling theorem. However, there is an issue of the waveform missing, when the sampling clock frequency has some relationships with the waveform repetitive frequency. There, it needs a lot of data and hence it takes a long time for the whole waveform reconstruction; its waveform acquisition is inefficient.

In this paper, we propose a golden ratio sampling for the efficient waveform acquisition, which can avoid the waveform missing phenomenon. Also its relationship with the golden section search algorithm is discussed. Then its applications as well as its limitation are discussed.

II. EQUIVALENT-TIME SAMPLING TECHNIQUE

Waveform sampling techniques can be classified into the real-time sampling and the equivalent-time sampling. The equivalent-time sampling techniques are used in a sampling oscilloscope for wideband signal measurement with a relatively low frequency sampling clock, and they can be classified into the sequential sampling and the random sampling [1-4]. We consider here the random sampling for a periodic waveform, where the sampling clock and the waveform can be incoherent or coherent. The sequential sampling can realize a highly efficient waveform acquisition but it does not acquire pre-

trigger waveform, while the random sampling can be inefficient when the measured waveform repetitive frequency and the sampling clock frequency are in some condition.

A. Random Sampling

The random sampling employs an asynchronous sampling clock for the measured waveform signal, and we consider the case that it is periodic and each sampling time from the phase zero of the measured waveform is measured and known. Then after many sampling data acquisitions, a waveform with one period can be reconstructed. Fig.1 shows the case that the input waveform is a sine wave (but the discussion here is not restricted to only the sine wave case).

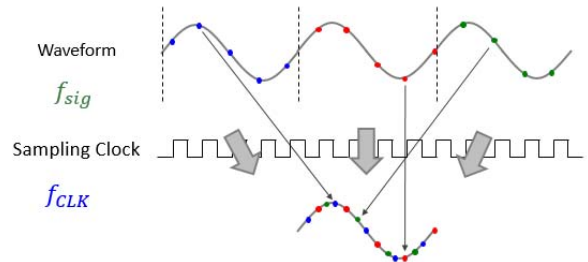


Fig. 1. Principle of Equivalent-time Sampling.

B. Waveform Missing Phenomena

Fig. 2 shows a typical development of a reconstructed waveform for the random sampling in a proper sampling condition. However, waveform missing phenomena, which require a long time to acquire a whole waveform of one period in the random sampling system may be caused in the following cases:

- 1) $f_{CLK} \gg f_{sig}$: The measured waveform repetitive frequency (f_{sig}) is very low compared the sampling clock frequency (f_{CLK}), as shown in Fig. 3.
- 2) $f_{CLK} \approx (1/\alpha) f_{sig}$: The measured waveform repetitive frequency (f_{sig}) is approximated to the harmonics of the sampling clock frequency (f_{CLK}), as shown in Fig. 4.

$$\alpha = 1, 1/2, 1/3, 2/3, \dots$$
- 3) $f_{CLK} \approx f_{sig}$: The measured waveform repetitive frequency (f_{sig}) is very close to the sampling clock frequency (f_{CLK}), as shown in Fig. 5.

Fig. 6 shows the waveform reconstruction comparison for the random sampling using 64 sampling points, and we understand waveform missing phenomena intuitively.

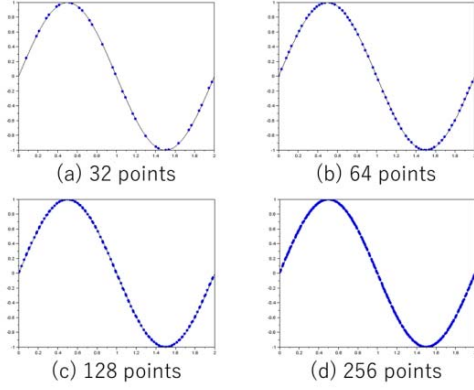


Fig. 2 Development of a reconstructed waveform for a random sampling

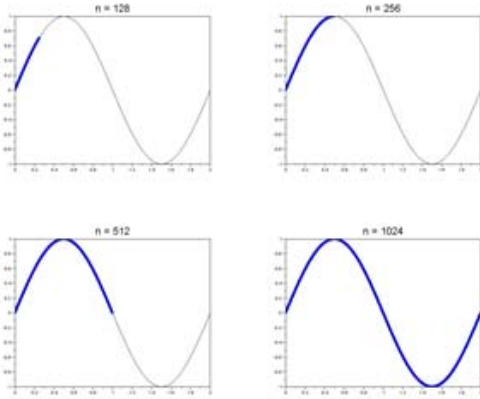


Fig. 3 Waveform missing phenomenon in case of $f_{CLK} \gg f_{sig}$

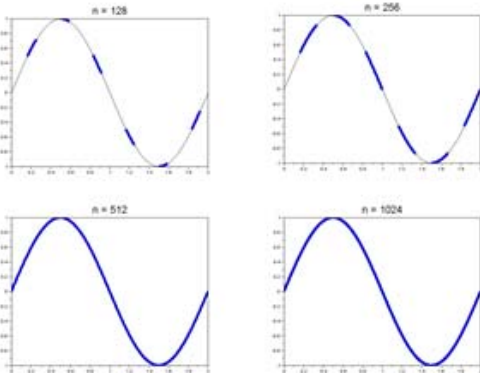


Fig. 4 Waveform phenomenon missing in case of $f_{CLK} \doteq (1/6) f_{sig}$

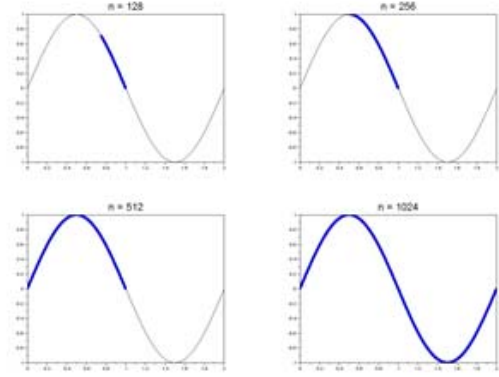


Fig. 5 Waveform missing phenomenon in case of $f_{CLK} \doteq f_{sig}$

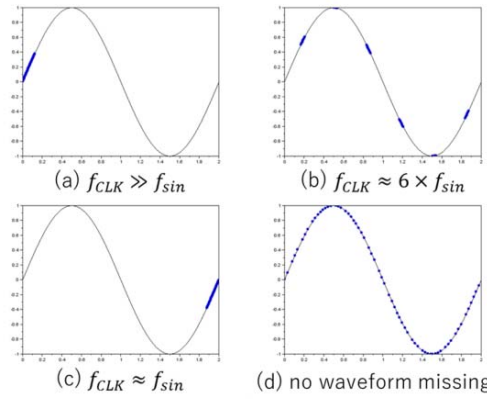


Fig. 6 Waveform reconstruction comparison for random sampling (64 points).

III. GOLDEN RATIO AND GOLDEN-SECTION SEARCH ALGORITHM

The golden section search algorithm is to obtain an extreme value of the unimodal function $f(x)$ efficiently [5, 6]. By comparing two function values, the extreme value can be obtained by narrowing the range successively (Fig. 7); this algorithm is known as the most efficient algorithm to find the extreme of the unimodal function. The range of the independent variable x has three points whose distance ratios are as follows:

$$\phi : 1 = 1 : \phi - 1 \quad (1)$$

It follows from Eq. (1) that

$$\phi^2 - \phi - 1 = 0 \quad (2)$$

Then we have the following:

$$\phi = \frac{1 + \sqrt{5}}{2} \approx 1.618 \dots \quad (3)$$

ϕ is known as the golden ratio and it has several properties as follows [5-7]:

- $\phi^2 = \phi + 1$ (4)

- $1/\phi = \phi - 1$ (5)

The merit of golden section search is that the narrowed range is greater than the one with the ternary search and its ratio is always constant. If the three points do not satisfy Eq. (2), some narrowed range will be smaller, and then the number of search times may increase. Another merit of the golden search is that the previous function value can be reused.

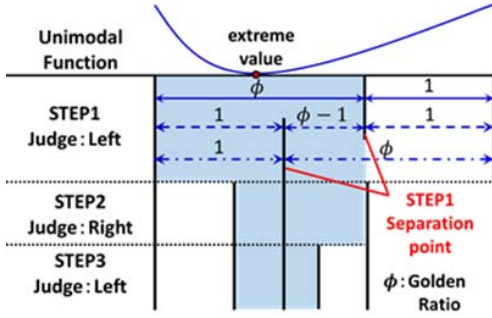


Fig. 7 Golden section search algorithm to find an extreme value of a unimodal function.

IV. PROPOSED GOLDEN RATIO SAMPLING

Fig. 8 shows the simulation result of our proposed golden ratio sampling ($f_{CLK} = \phi f_{sig}$) with 16 points from the phase zero of the input waveform. The period of the input signal is normalized as 1 and that of the sampling clock is $1/\phi$. Their rate is $\phi:1$, which we call the golden ratio sampling. Then, although the Nyquist sampling theorem is violated, the input waveform can be reconstructed from the sampled points because the input signal is repetitive and the equivalent-time sampling is employed. Table I shows their phases and their distances. We see from Fig. 8 that waveform missing is not observed and an efficient waveform acquisition is obtained.

This can be explained with the golden section search algorithm. We see from Table I that the order of the sampling point phases in Fig. 8 is similar to the ones with the golden section search in Fig. 7 when the start phase is set appropriately.

A. Phase distance between successive sampling points

The normalized phase distances between previous and present sampling points are always $1/\phi$ ($=0.618$) or $1/\phi^2$ ($=0.382$) as shown in Table I. This means that the interval between the previous and present points must apart by a constant, and never be close. Thus, sampling points disperse across the period of the input signal.

Fig. 9 shows the maximum and minimum steps to the next point versus total number of acquisition data (N_s), where $f_{sig} = 1$, $f_{CLK} = \phi$. There, both steps decrease by $1/\phi$ every which can be explained by Fibonacci numbers. As the result, they decrease by about $1/N_s$. We consider that it is the repetitive golden-section search of every divided section. With the golden ratio sampling, the time resolution improves by $1/N$.

In the case of the sampling at random, the time resolution improves by $1/N_s$. Thus we see that the golden ratio sampling realizes highly efficient data acquisition for the equivalent-time sampling system.

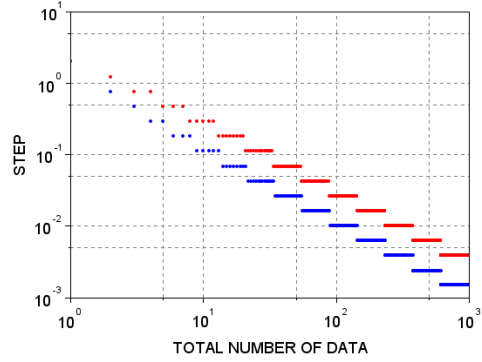


Fig. 9 Maximum and minimum steps in the golden-ratio sampling.

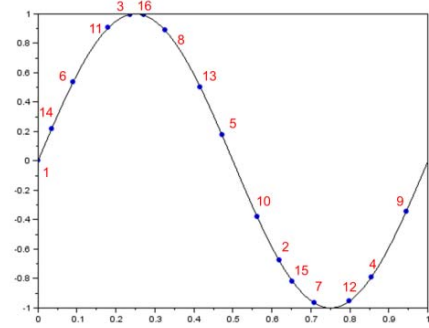


Fig. 8 The sampling order with the golden ratio sampling starting from phase 0 (16 points).

B. Simulation Results

We show simulation results for the histogram of the sampling points generated by the proposed golden ratio sampling rate in Fig. 10. This is the result after 1000-point acquisition and the horizontal axis indicated the phase of the sampled point, which is normalized from $0 \sim 2\pi$ to $0 \sim 1$. The sampling points disperse uniformly as the standard deviation of the histogram is sufficiently small (0.0004).

Fig. 11 shows the standard deviation change of the histogram over the number of the total sampling data (N). Here the standard deviation σ is defined as

$$\sqrt{(\sum ([\text{the histogram data} - \text{the uniform histogram data}]^2) / B)}$$

B: number of bins.

In Fig. 11, the blue dots show the simulated standard deviation for each N , and the red line indicates their fitting curve. The standard deviation decreases rapidly as N increases; it is proportional to $N^{-0.92}$. This means that the sampled points move randomly and stay uniformly.

Next, we consider the integral randomness of the phases of the sampled points. Fig. 12 shows the accumulated histogram in Fig. 10, where the previous normalized count (histogram data) is accumulated to next bins and for the phase 1.0 of the horizontal axis, 1.0 of the vertical axis is provided. We search its root-mean-square (RMS) value versus number of data. Here the standard deviation σ is defined as

$$\sqrt{(\sum ([\text{the accumulated histogram data} - \text{the linear accumulated histogram data}]^2) / B).$$

B: number of bins.

In other words, Fig. 10 shows the differential nonlinearity (DNL) while Fig. 12 shows the integral nonlinearity (INL) of the sampled data phases.

Fig. 13 shows the INL standard deviation change in Fig. 12 in case of the golden ratio sampling, with respect to the number of the total sampling data. The blue dots show the INL standard deviation obtained by simulation and the red line indicates their fitting line. The INL standard deviation decreases as the number (N) of the total data increases, which is proportional to $N^{-0.95}$. The steep incline means uniformness and less oscillation means randomness.

To find the optimal sampling frequency which minimizes the INL standard deviation with respect to the number (N) of the total data, we have simulated using the various relationships between the sampling clock and input signal frequencies, as shown in Eq. (6).

$$f_{sig} = \frac{Q}{P} f_{CLK} \quad (6)$$

(where P and Q are integers and relatively prime.)

P is the maximum number of the total measurable sampled phases, whereas Q determines the phase distance for each sampling. The simulation results are shown in Fig.14, where the RMS value of the INL standard deviation from the fitting curve with respect to Q for P=1024 and N=1000. Here the RMS is defined as

$$\sqrt{(\sum ([\text{the blue dot data} - \text{the fitting red curve}]^2) / N).$$

In Fig. 14, the horizontal axis indicates Q where the vertical axis shows RMS. The RMS becomes minimum at Q = 637 and it is second minimum at Q=397 (Fig.15). Notice that $1024/637=1.6075..$ and $1024/(1024-397) =1.633...:$ they are nearly equal to $\phi=1.618$, and we see that the optimum sampling condition is related to the golden ratio.

Remark:

(i) The fact that the RMS is small means that the sampled phase is uniform as well as random. Then the results in Fig. 8 and Fig.15 show that the golden ratio sampling acquires the waveform randomly and uniformly in phase, and the waveform missing does not occur.

(ii) Even when the approximate golden ratio sampling, for instance 1.1618 and 1.6181, is used, the waveform missing does not occur; so the golden ratio sampling condition is robust for no waveform missing.

(iii) The maximum number of the sampling points depends on whether the sampling clock and the input signal are synchronous. For example, suppose that an input signal clock period is 1.0 and the sampling clock period is 0.618 (hence they are synchronous), then the maximum number of the sampling points is 500[points] as $0.618 = 618/1000 = 309/500$. After 500 times acquisition, you cannot obtain further data with new phases. In other words, the frequency ratio between the input signal and the sampling clock has to be an irrational number (in other words, both are asynchronous) for data acquisition with many phases.

TABLE I. SAMPLED PHASES AND THEIR GAPS (FIG. 8)

No.	Phase	Phase Distance	Max. Step	Min. Step
1	0.000	0.618	1	1
2	0.618		0.382	0.618
3	0.236	0.618		0.382
4	0.854		0.382	0.382
5	0.472	0.382		0.236
6	0.090		0.618	0.236
7	0.708	0.382		0.236
8	0.326		0.618	0.146
9	0.944	0.382		0.146
10	0.562		0.382	0.146
11	0.180	0.618		0.146
12	0.798		0.382	0.146
13	0.416	0.382		0.090
14	0.034		0.618	0.090
15	0.652	0.381		0.090
16	0.271			0.090

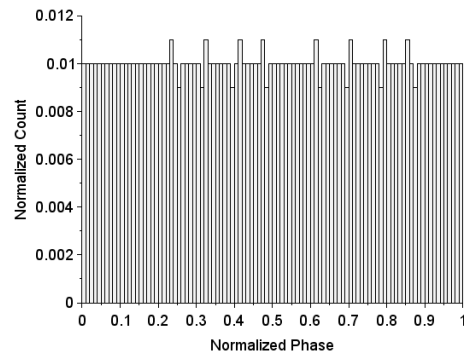


Fig. 10 The histogram of the data obtained using the golden ratio sampling clock (1000 points).

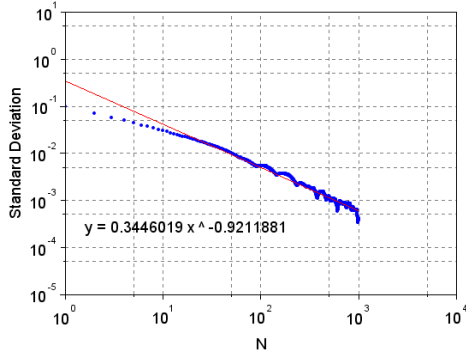


Fig. 11 DNL standard deviation change of the histogram versus the number of the total sampled data N (golden ratio sampling case).

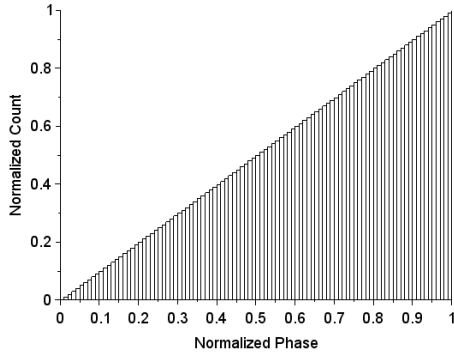


Fig. 12 Accumulated histogram of the sampling data obtained using the golden ratio sampling clock (N=1000 points).

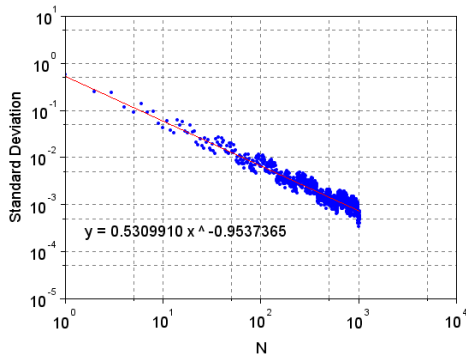


Fig. 13 INL standard deviation change in Fig.11 versus the number of the total sampling data (golden ratio sampling case).

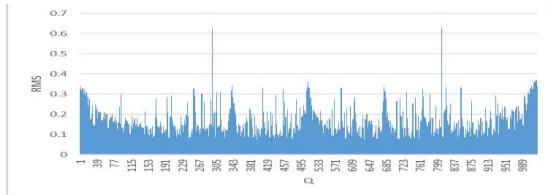


Fig. 14 RMS from the approximate curve versus the frequency (Q) for P=1024.

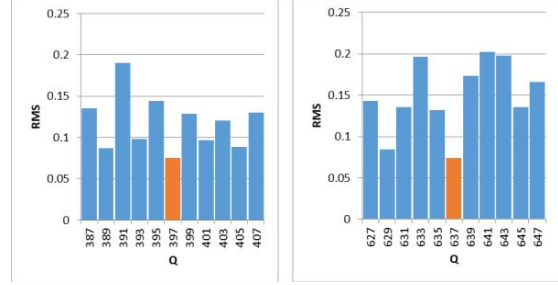


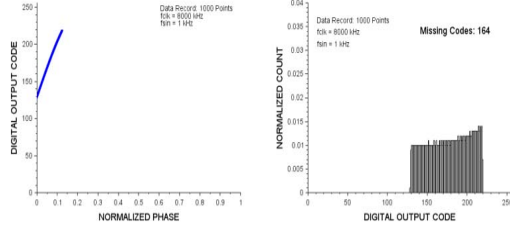
Fig. 15 Enlarged views of Fig. 13.
 (Left) The RMS is second minimum at Q=397. P/(P-Q)= 1.633..
 (Right): The RMS is minimum at Q=637. P/Q= 1.607...

V. DISCUSSION

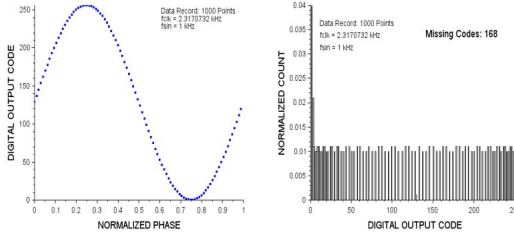
In this paper, we have investigated the golden ratio sampling and we consider that this can be applied to LSI testing and measurement technologies as follows:

- (1) Wideband Waveform Sampling Systems: if the input signal is repetitive and its period is known, its efficient waveform acquisition with equivalent-time sampling is realized by employment of the adjustment function for the sampling clock frequency using the golden ratio, so that the waveform missing phenomena are not caused.
- (2) ADC Testing with Histogram Method: The histogram method with a sine wave input is widely used for ADC testing [8]. For its given sampling clock frequency, its input frequency can be chosen to obtain the histogram data efficiently with relatively small number of data. We see in Fig. 16 that the histogram test in waveform missing cases does not work properly, while it works well in case of golden ratio sampling; DNL and INL of the ADC can be measured accurately. Fig. 17 shows the DNL simulation result that compares golden-ratio sampling and sampling at random.
- (3) Time-to-Digital Converter Calibration: Non-linearity of a flash-type time-to-digital converter can be calibrated by applying two asynchronous clocks to two inputs and obtaining the histogram of its output data [9]. If the ratio of their frequencies is related to the golden ratio, then the calibration may be performed effectively.
- (4) Integral-type Time-to-Digital Converter: A high performance integral-type time-to-digital converter which uses two clocks can be realized if their frequency ration is the golden-ratio. A part of it is described in [10] and its details will be reported elsewhere.

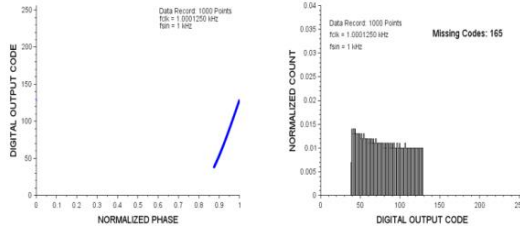
The limitation of the proposed sampling technique is the following: Two repetitive signals with different frequencies are used, and one of its repetitive frequency should be known so that the other frequency should be adjusted/controlled.



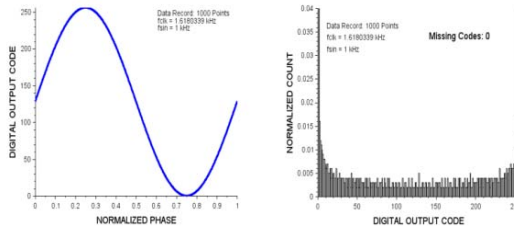
(a) In case of $f_{CLK} \gg f_{sig}$



(b) In case of $f_{CLK} = (1/\alpha) f_{sig}$



(c) In case of $f_{CLK} \div f_{sig}$



(d) Golden ratio sampling case

Fig.16 ADC histogram sampling in waveform missing cases and golden ratio case with 1,000 points.

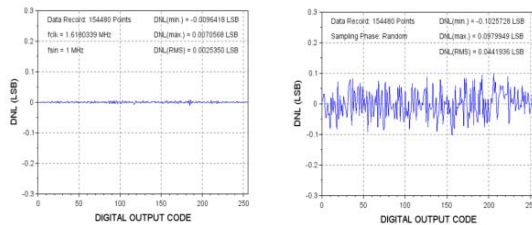


Fig.17 ADC histogram test of DNL with 154,480 points, 8bit
(Left) Golden-ratio sampling (Right) at Random

VI. CONCLUSION

In this paper, efficient sampling techniques for equivalent-time sampling have been presented. With our proposed golden ratio sampling rate, waveform missing phenomena do not occur and an order of the sampling points is arranged in a pseudo random manner. Thus, the sampling timing for the waveform acquisition disperses over one period of the measurement waveform. The proposed technique can be used for equivalent-time sampling systems and ADC testing with the histogram method, as well as time-to-digital converter calibration and design.

We conclude this paper by remarking that beautiful mathematics such as golden ratio leads to sophisticated analog/mixed-signal IC design and testing [11, 12].

ACKNOWLEDGEMENT

The authors would like to thank K. Sato, T. Nakatani, K. Hatayama, and Y. Kobori for valuable discussions. Thanks are also due to ROHM Co., Ltd. for kind support of this project.

REFERENCES

- [1] D. E. Toeppen, "Acquisition Clock Dithering in a Digital Oscilloscope," Hewlett-Packard Journal, vol. 48, No. 2, pp. 26-28, April 1997.
- [2] K. Rush, D. J. Oldfield "A Data Acquisition System for 1-GHz Digitizing Oscilloscope," Hewlett-Packard Journal, vol. 37, No. 4, pp. 4-11, April 1986.
- [3] M. Kimura, A. Minegishi, K. Kobayashi, and H. Kobayashi, "A New Coherent Sampling System with a Triggered Time Interpolation," IEICE Trans. on Fundamentals, vol. E84-A, no. 3, pp.713-719 (March 2001).
- [4] M. Kimura, K. Kobayashi and H. Kobayashi, "A Quasi-Coherent Sampling Method for Wideband Data Acquisition", IEICE Trans. on Fundamentals, vol. E85-A, no. 4, pp.757-763, (April 2002).
- [5] W. H. Press, S. A. Teukolsky, W. T. Vetterling, B. P. Flannery, "Golden Section Search in One Dimension", Numerical Recipes: The Art of Scientific Computing (3rd ed.), in Section 10.2, Cambridge University Press (2007).
- [6] H. Arai, T. Arafune, S. Shibuya, Y. Kobayashi, K. Asami, H. Kobayashi, "Redundant SAR ADC Algorithm for Minut Current Measurement", International Conference on Mechanical, Electrical and Medical Intelligent System, Kiryu, Japan (Nov. 2017).
- [7] Y. Kobayashi, S. Shibuya, T. Arafune, S. Sasaki, H. Kobayashi, "SAR ADC Design Using Golden Ratio Weight Algorithm", The 15th International Symposium on Communications and Information Technologies, Nara, Japan (Oct. 2015).
- [8] F. Maloberti, Data Converters, Springer (2007)
- [9] S. Ito, S. Nishimura, H. Kobayashi, S. Uemori, Y. Tan, N. Takai, T. J. Yamaguchi, K. Niitsu, "Stochastic TDC Architecture with Self-Calibration," IEEE Asia Pacific Conference on Circuits and Systems, Kuala Lumpur, Malaysia (Dec. 2010).
- [10] Y. Sasaki, H. Kobayashi, "Integral-type Time-to-Digital Converter and its Optimal Sampling Clock Frequency," IEEE Workshop, Kiryu, Japan (March 2018).
- [11] H. Kobayashi, "Analog / Mixed-Signal IC Design and Testing Based on Mathematics", 2nd International Conference on Technology and Social Science, Kiryu, Japan (April, 2018).
- [12] H. Kobayashi, H. Lin, "Analog / Mixed-Signal Circuit Design Based on Mathematics", IEEE 13th International Conference on Solid-State and Integrated Circuit Technology, Hangzhou, China (Oct. 2016)